RANKING OF UNCERTAIN PARAMETERS FOR DYNAMIC EVENT TREE ANALYSIS: A CASE STUDY BASED ON A STATION BLACKOUT SCENARIO

S. Rahman[*1], D. R. Karanki[2], A. Epiney[1], O. Zerkak[1] and V. N. Dang[2]
1) Laboratory for Reactor Physics and Systems Behavior
2) Laboratory for Energy Systems Analysis
Paul Scherrer Institut
5232 Villigen, Switzerland
*saidur.rahman@psi.ch

ABSTRACT

Dynamic Event Tree analysis which couples thermal-hydraulic system models with safety system and operator response models is a realistic but computationally challenging approach for risk quantification in nuclear power plants. Dynamic Event Tree analysis should also include a framework to quantify uncertainty due to the relevant aleatory and epistemic parameters of the risk assessment model. Since the computational requirements do not scale well with the number of uncertain parameters, a first necessity is to reduce the number of parameters through a rigorous selection process based on sensitivity analysis.

A first step in this direction is made in this work, which presents an exemplary parameter ranking study based on a Station Black Out scenario of a Pressurized Water Reactor design (Zion power plant). Thus, a Zion power plant model for Station Black Out analysis using the TRACE thermal-hydraulic system code is employed together with Pearson and Spearman correlation coefficient methods in order to rank thirteen uncertain parameters preliminarily selected from own judgment. The candidate parameters include initial and boundary (I/B) conditions for the core (e.g. initial power, decay heat, axial core power distribution) and for the system (e.g. steam generator secondary mass inventory, water level in accumulators) as well as four physical parameters (wall to vapor heat transfer coefficient, nucleate boiling heat transfer coefficient, interfacial drag in bubbly and pre-critical-heat-flux flow regimes) that are ranked according to their correlation with core damage frequency within the validity domain of the model (no-core melt).

As a result of the study based on 158 realizations of the simplified core damage frequency estimate model, the interfacial drag (pre-critical-heat-flux regime), the axial power offset and the steam generator liquid mass inventory are the high rank parameters as identified by both Pearson and Spearman correlation coefficient methods. However, both methods failed to identify another dominant contributor that is the initial water volume in the accumulators. The reason is that neither Pearson nor Spearman can capture the contribution to the output of cross interactions between the input parameters. But in this scenario the intricate interaction of the accumulator with the primary system during the intermittent passive injection phase is shown to have a non-negligible impact on the distribution of the core failure probability. This result hints at non-linear interactions between the parameters of the risk model, and shows the limits of sensitivity analysis methods based on linear or monotonic correlation coefficients.

KEYWORDS
Thermal Hydraulics, Sensitivity Analysis, Dynamic Event Trees, PSA

1. INTRODUCTION

Nuclear Power Plants (NPPs) can be subject to plant modifications to achieve lifetime extension beyond the initial approved licensing periods or to enhance economic performance such as extended power up-rates and/or increased fuel burn up [1]. These modifications (not necessarily or completely considered in the original design) can affect the safety characteristics in case of accidents. Then questions logically arise with respect to whether a potential increase to the risk (core damage frequency (CDF)) may result and whether the plant's safety margins remain adequate [2-3].

In order to evaluate the safety margin a basic requirement is to know the uncertainty associated with the risk estimate. In a typical accident scenario of a NPP, complex dynamic interactions are present between the physical processes and safety systems responses. Therefore, uncertainties in physical models as well as in the parameters of the probabilistic response models need to be quantified. To do so, one approach is a Dynamic Event Tree (DET) tool coupled with a NPP simulation model [4-5]. In this framework, the integrated simulations of the accident scenario generate the sequences and then the risk is computed based on the outcome of the sequences and the probability of the initiating events. The integrated modeling of physical process and failure response supports the propagation of physical model parameter uncertainties, which is usually circumvented in current PSA methods by combining diverse conservative assumptions.

The DET can also provide a more realistic approach by adding the uncertainty in physical process simulation parameters (epistemic) to the other parameters (epistemic and aleatory) of the risk model. However the propagation of uncertainties in a DET is a challenge, since the set of uncertain parameters is often very large and the computational cost of each run can be significant (thousands of seconds of simulated time).

To overcome the computational burden an alternative approach is to build a fast-running surrogate regression model (e.g. response surface) in order to approximate the input/output function of the real process simulation model [6-7]. However, the construction of such regression models requires significant model calibration efforts and the issue boils down again to the computation efficacy. Moreover, it is known that the fewer the number of input parameters, the better the accuracy with response surface methods, hence the need in any case to reduce the number of meaningful parameters to the minimum.

In this context, a first step is to use sensitivity analysis in order to rank and select the important uncertain parameters from the set of candidate parameters preliminary selected by own judgment. The candidate parameters can include I/B conditions as well as input and physical model parameters, which are ranked according to their influence on relevant safety criteria (e.g. cladding temperatures), so that only the significant contributors can be selected for regression analysis.

The Station Blackout (SBO) accident scenario (one of the dominant contributors to the CDF estimate) of the Zion power plant has been chosen as the case study. The SBO sequence involving loss of auxiliary feed water system (AFWS) followed by failure to recover power supply for Feed and Bleed (FB) has been selected for the detailed sensitivity analysis. Sequence simulations are performed using the best estimate code TRACE (TRAC/RELAP Advanced Computational Engine) [8]. Section 2 presents the main assumptions of the reference sequence, and describes the different components of the risk model. Section 3 discusses the simulation results for the reference sequence and presents the parameters of the sensitivity analysis. Section 4, briefly describes the ranking method used, based on Pearson and Spearman correlation coefficient methods, and further discusses the impact of the different parameters on the CDF.

2. DESCRIPTION OF SBO ACCIDENT SEQUENCE AND RISK MODEL

The SBO accident is often the most important contributor to the CDF of a nuclear reactor. SBO denotes loss of offsite power supply (external grid) coupled with loss of onsite emergency power supply (using diesel generator) crippling core coolant flow, including the emergency core cooling system. This condition actuates turbine driven AFWS that ensures core cooling through secondary side heat removal. In case of unavailability of AFWS, recovery of power supply is necessary to initiate FB which will prevent core damage. The FB involves operator action on the power operated relief valves (PORV) of the pressurizer (PZR) to depressurize the primary and inject the coolant by one of the safety injection trains into the reactor coolant system. The recovery time of power supply and operator response to FB action are critical events that determine the outcome of the SBO accident scenario. The high pressure condition on the primary side can lead to a main coolant pump seal loss of coolant (LOCA), where power recovery and FB are also necessary.

2.1. Reference Accident Sequence

An SBO sequence involving loss of AFWS followed by failure to recover power supply for FB operation has been considered for this case study. The sequence path for this event is shown in Fig. 1 as considered by the CSNI task group SM2A at the OECD/NEA [9] after screening and modifying the LOSP (Loss of Offsite Power) PSA event tree described in [10].
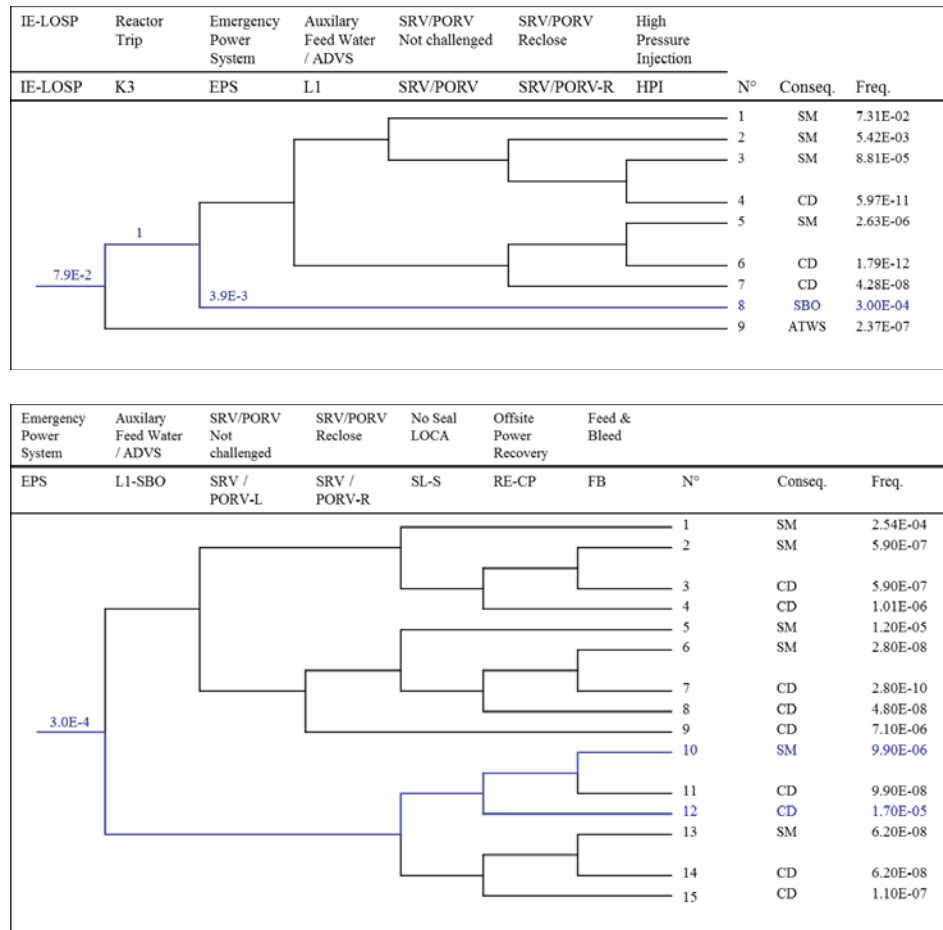

Figure 1. Loss of offsite power event tree (top); SBO accident sequence event tree (bottom) [9-10].

The reference sequence 12 starts with a transient initiated by turbine trip due to a loss of offsite power. In response to the turbine trip the reactor scram should be generated automatically. To pick up all required safety load, emergency power supply (e.g. diesel generator) is demanded. In this sequence, emergency diesel generators fail to operate on demand. Normally, the turbine-driven auxiliary feed water (AFW) pumps should be started since feed water pumps would be unavailable. However, in this sequence also the AFW pump fails to operate, turning the sequence into an SBO with loss of AFW. Following the no pump seal LOCA condition, core cooling should be provided by FB process. In the top event FB, it is required that the operator manually opens the pressurizer PORVs to provide bleed path and actuation of at least one high head safety injection pump to provide the feed. Thus, successful FB requires operator action to provide bleed path as well as AC power recovery to actuate the safety injection before core uncover. The cue for operator for bleed actions comes from the low level in the steam generators (SGs), which is due to loss of inventory from auto opening of the SG PORV. A delay of 20 minutes for operator action is assumed in the current analysis. Subsequently, depressurization of primary due to bleed action results in accumulators' injection, which are assumed to be available. In the reference sequence (12), failure to recover power supply is considered, which leads to core damage due to lack of safety injection.

2.2. Risk Model

The initial event frequency of SBO and the failure probability of each heading related to FB transient are listed in Table I.

Table I. Initial events and failure probabilities (source [9-10]).

Event	Description	Probability
IE-LOSP	Initial event	7.9E-2
EPS	Emergency Power System	3.9E-3
L1-SBO	Auxiliary Feed Water	8.9E-2
SL-S	Main Coolant Pump Seal LOCA	6.3E-3
RE-OP	Offsite Power Recovery	6.3E-1
FB	Feed and Bleed	1.0E-2

In the analyzed FB sequence, safety injection (or electrical power recovery) is not explicitly considered. It is known that an early recovery avoids core damage, whereas a late recovery leads to core damage. These recovery times may vary from a few minutes to several hours. Fouet et al. [2] proposed to use an exponential law to calculate the failure probability of power recovery (P_{FPR}) as

$$P_{FPR}(t) = \exp\left(\frac{-t}{\tau}\right) \tag{1}$$

Where t is the power recovery delay expressed in hours and τ is the mean value (1 hour for this study).

As shown in Fig. 2, recovery of the power supply a few minutes (10 minutes in [2]) before PCT reaches 1477 K would make safety injection successful in preventing core damage. This latest time (t) for recovery of power supply to prevent core damage is used in equation (1) to determine failure probability of power recovery. The CDF of the reference sequence is then evaluated considering recovery failure probability and SBO frequency. This approach, as indicated by Fouet et al. [2], helps reducing the number of sequences to be simulated as the need for the discretization/sampling of the power recovery in the DET model of the sequence is eliminated.
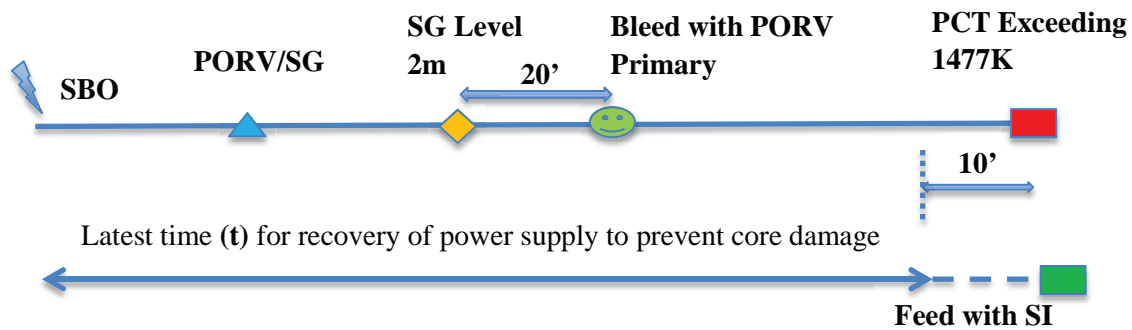
Figure 2. Important events in the reference sequence and their relationship with recovery time.

2.3. Thermal Hydraulic Model

2.3.1. Transient analysis code TRACE

In this study, the system code TRACE V5.0 P03 [8] has been used for the TH simulations. TRACE is the best-estimate TH code developed by the U.S. Nuclear Regulatory Commission (USNRC) for steady-state and transient analysis of light water reactors.

2.3.2. Model Nodalization

The TRACE input deck of the Zion reactor, developed within the BEMUSE project (Best Estimate Methods for Uncertainty and Sensitivity Evaluation) Phase IV [11], has been adapted for this case study. The TRACE nodalization of the Zion reactor uses one dimensional components except for the reactor pressure vessel, which is modeled with a three-dimensional component. A schematic of the nodalization is shown in Fig. 3. Pink colored components have connections to heat structures (HTSTR), green colored components have connections to powered HTSTR while yellow components have no HTSTR.

The nodalization consists of 208 hydraulic components, 78 heat structures and 218 control blocks. The four loops, including the SGs, are modeled separately. The reactor pressure vessel consists of 4 azimuthal sections, 6 radial rings, and 27 axial levels. The reactor core is composed of 4 radial rings and 18 axial levels. The fifth and sixth rings represent the core bypass and downcomer, respectively. The power component is thermally linked to the core section of the vessel component using four heat structures.

Compared to the original model from the BEMUSE Phase IV project, the Pressurizer safety valve and PORV of the pressurizer and their corresponding break boundary condition components have been introduced in the model as shown in Fig. 3. The nodalization and connection junctions to the pressurizer of the two added valves follow the best-practice modelling guidelines from the U.S. NRC [12]. Thus, since no geometry information for these two valves were available, zero cell valve components have been used for both valves. The characteristics of the valve flow such as valve opening set pressure and flow area have been defined on the basis of information in [2]. Special effort has also been spent in revising the accumulator tank and injection line nodalizations in line with the guidelines in [12], except for the accumulator model option. The suggested latest available option (IACC = 2) has not be retained and the base accumulator model option has been used instead (IACC = 1).
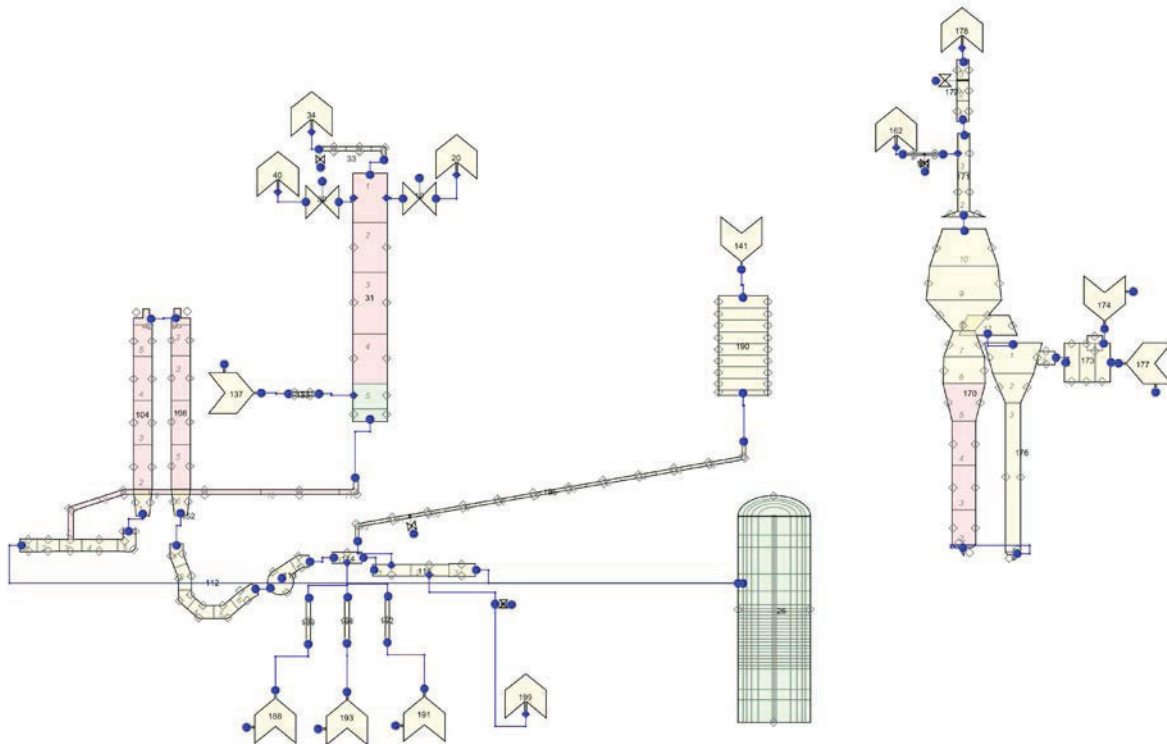
Figure 3. TRACE nodalization of the Zion reactor (one loop representation).

2.3.3. Steady state results

In order to verify the TRACE nodalization of the Zion reactor, TRACE steady state results have been compared to the CATHARE results reported in [2] for the analysis of the same system and scenario. The comparison of the steady state values for the two codes is presented in Table II. As can be seen, the steady state results from TRACE and Ref. [2] are in a sufficiently good agreement for the purpose of this study (SG liquid mass inventories are close, primary temperatures hint at similar primary mass inventories).

Table II. Comparison of TRACE steady state results and Ref. [2] results for the Zion reactor.

	[Units]	**TRACE**	**Ref. [2]**
Primary side			
Power	MW$_{th}$	3250	3250
Pressurizer pressure	MPa	15.5	15.5
Cold leg temperature	K	555	550
Hot leg temperature	K	589.5	585
Core flow	Kg/s	17315	17340
Secondary side			
Steam generator pressure	MPa	5.16	5.15
Steam generator level	m	12.9	-
Steam generator inventory	ton	47.2	48
Secondary side feedwater flow	Kg/s	440.8	443
Secondary side feed water temperature	K	493.45	493.4

3. REFERENCE CASE AND CANDIDATE PARAMETERS FOR SENSITIVITY ANALYSIS

3.1. Reference Case

3.1.1. Analysis assumptions and boundary conditions

The main analysis assumptions and boundary conditions for the FB sequence are listed in Table III.

Table III. Main analysis assumptions of the FB sequence.

Description of actions	Assumptions
Loss of Feed water and reactor trip	at t = 0 s
Reactor scram	at t = 1.2 s
Opening of SG PORV	P_{SG} = 61 bar
Pressurizer safety valve setpoints	P > 166 bar (valve flow area = 15 cm^2) P < 160 bar (valve flow area = 0 cm^2)
FB through pressurizer PORVs	ΔP_{SG} < 0.14 bar & Level$_{SG}$(collapsed) = 2 m; PORVs flow area = 45 cm^2 Operator action delay : 20 minutes
Accumulators opening /closing	P_{PZR} < 41 bar / P_{PZR} < 15 bar

3.1.2. Simulation results for the reference case

The transient starts with a loss of feed water resulting in a reactor trip. This generates reactor scram and a trip of the reactor coolant pumps and the main feed water pumps. The heat sink for this transient is the water initially present in the SGs. Since no AFW supply is available, the water in the SG is boiling off as decay heat is transferred from primary to secondary side (Fig. 4 (top)). The pressure in the SG reaches the SG PORVs actuation set point (61 bar) within few seconds. Opening of the SG PORVs (automatically open when the pressure set point is reached) limits further pressure increase in the secondary side but liquid water inventory of the SGs is lost through the PORVs. During this phase, the primary side is experiencing quasi-steady decay heat removal by natural circulation, which transfers the core excess heat to the secondary side of the SGs. The SG mass inventory keeps being vented in form of steam through the PORVs until the water level has reached 2 m level (in the calculation at 1500 s). At this point, the operator has a cue to open the bleed path. The reference case assumes a 20 minutes delay for the operator to actuate the bleed path.

The pressurizer PORVs open (bleed path by the operator action) in the simulation at about 2700 s as can be seen in Fig. 4 (top). In the risk model we do not model explicitly the safety injection after power recovery. Therefore, accumulators are the only source of emergency core cooling. The primary coolant mass inventory is discharged through the pressurizer PORVs and the core level starts to decrease. Subsequently, the system pressure drops below the accumulator injection set point pressure of 41 bars at about 4980 s (Fig. 4 (bottom)). The accumulator injection replenishes the mass inventory in the primary circuit until 6250 s (Fig. 4 (bottom)) and then the accumulator injection is intermittent depending on the pressure difference between the accumulator and the primary system (this is discussed in more details in section 4.2.2). Later on, the accumulators are nearly empty and the core uncovers again. The Peak Cladding Temperature (PCT) reaches the maximum allowable value of 1477 K at about 8100 s, as can be seen in Fig. 4 (bottom).
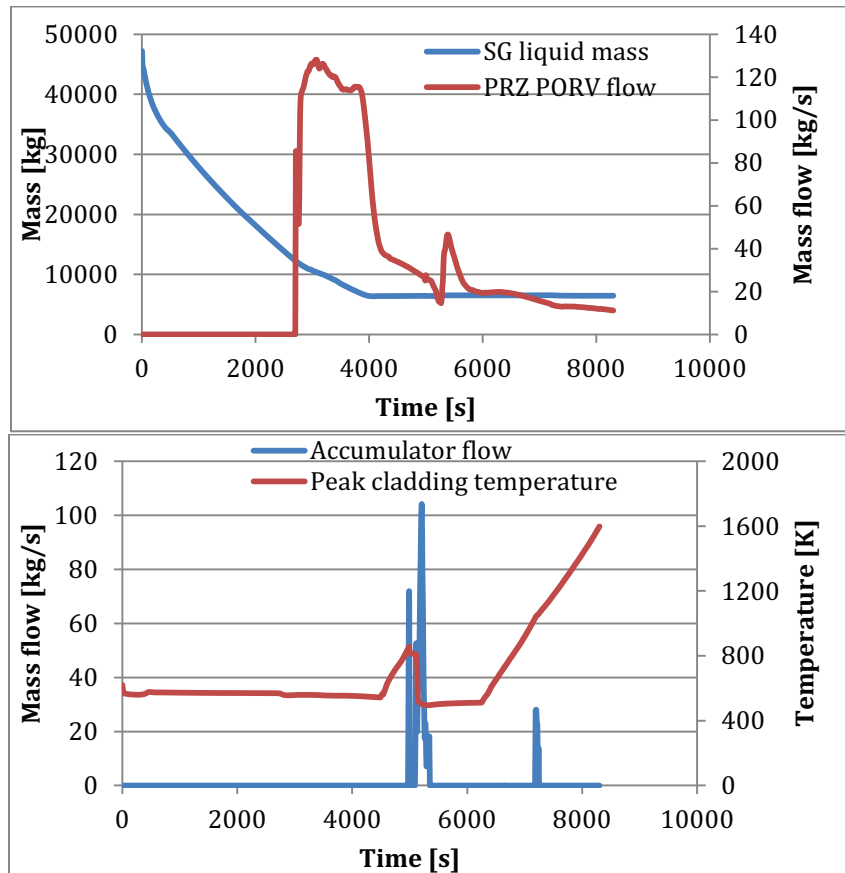
Figure 4. TRACE simulation results for the reference case.

3.2. Specification of Uncertain Candidate Parameters

With respect to the FB sequence, two types of uncertain parameters are considered in the present study. These are the I/B condition parameters and physical model parameters as listed in Table IV. The I/B condition uncertain parameters and their ranges that have been identified and selected in the frame of SM2A exercise [2] have been re-conducted here, with the addition of the axial power offset. The axial power offset varies from -30% to +30%. The axial power distribution as function of the axial power offset has been derived using a simple analytical expression as proposed by Tochihara [13]. The radial power distribution has been taken from the specifications for Phase IV of the OECD/NEA BEMUSE project [11] and is assumed to be constant. The four physical parameters have been selected for their potential impact on relevant quantities of the problem, namely the liquid inventory in the primary system and the core cladding temperatures, hence:

- The interfacial drag coefficient in pre-CHF flow regime for its expected impact on the liquid entrainment up to the pressurizer PORV (through the hot legs, the surge line and the pressurizer),

- The interfacial drag coefficient in bubbly flow regime for its expected impact on the core water level swell during the core boil-off phase,

- The nucleate boiling HTC and the wall to steam HTC for their potential contribution to the heat transfer from the fuel rods to the coolant below and above the mixture level, respectively.

The uncertainty bands of the physical model parameters have been determined arbitrarily, but are deemed plausible in the limited context of this case study, noting also that two-phase flow closure models are known to be affected by significant epistemic uncertainty when employed for transient conditions.

Table IV: Uncertain parameters and their bounds.

Parameters	Variation range	Distribution
Initial and boundary conditions		
Decay power	ANS-79 ± 5%	Uniform
SG initial liquid mass	47 tons ± 5 tons	Uniform
Initial water volume of accumulators	23.8 m3 ± 10%	Uniform
Pressure loss coefficients of accumulators	K-factor x [0.5 ; 2]	Uniform
Initial power	100% ± 2%	Uniform
SG PORV set pressure	61 bar ± 2 bar	Uniform
Pressurizer safety valve section	15 cm2 ± 10%	Uniform
Feed and Bleed actuation delay	[20 min ; 30 min]	Uniform
Axial power offset	[-30% ; +30%]	Uniform
Physical model parameters		
Wall to vapor heat transfer coefficent	vwht x [0.5, 2.0]	Uniform
Interfacial drag coefficient in bubbly flow regime	bfid x [0.5, 2.0]	Uniform
Nucleate boiling heat transfer coefficient	nbht x [0.5, 2.0]	Uniform
Pre CHF interfacial drag coefficient	chfid x [0.5, 2.0]	Uniform

4. SENSITIVITY ANALYSIS

The relevant question for the sensitivity analysis is to explore how the uncertainties in the input parameters affect the available time window of SI recovery and consequently the core damage frequency, and thus to identify the most influential parameters among the previously selected candidates.

4.1. Methodology

The methodology is based on a sensitivity analysis applied to results from series of model executions in which the parameters uncertainties have been propagated by MC method. Samples of uncertain parameters are independently and randomly drawn from the distributions describing the uncertainties listed in Table IV. Each sample characterizes the model parameters for a single code run. For a given sample, input preparation is automated by utilizing Perl scripting. Essentially: a standard TRACE input deck is prepared by replacing input variables of interest as necessary according to the random draws from the uncertainty distributions, which acts as input to the script. Simulations are executed in batch mode on a Linux cluster.

Two statistics are used to rank the uncertain parameters, namely the Pearson product-moment correlation coefficient and the Spearman's rank correlation coefficient. The first coefficient is calculated using the sampled output values and the corresponding input values of the uncertain parameter of interest. Considering m samples from the output of interest and the uncertain parameter, denoted as y_j and x_j, for $j = 1$ to m, the Pearson correlation coefficient is computed from [14] as follows:

$$r_{XY} = \frac{\sum_{j=1}^{m}(x_j - \bar{x})(y_j - \bar{y})}{\sqrt{\sum_{j=1}^{m}(x_j - \bar{x})^2 \times \sum_{j=1}^{m}(y_j - \bar{y})^2}} \tag{2}$$

To calculate the Spearman correlation coefficient the m values of x_i, y_i are converted to ranks X_i, Y_i and the correlation coefficient ρ is computed using the following expression:

$$\rho = 1 - \frac{6 \sum d_i^2}{m(m^2-1)} \tag{3}$$

where $d_i = X_i - Y_i$, is the difference between ranks.

These correlation coefficients essentially provide an estimate of the degree of linearity or monotony in the relationship between the sample values of the model output and the input parameters. The value of r_{XY} or ρ lies between -1 to +1. The sign of the coefficient tells about the direction of the relationship, and the absolute value of the coefficient indicates the strength of the relationship where -1 indicates a completely negative linear correlation and +1 a completely positive linear correlation.

4.2. Results and Discussion

4.2.1. Evaluation of the core damage frequency

We used 158 random samples for the evaluation of core damage frequency. Statistical tests show that a fairly stable mean and standard deviation of the failure probability (associated 90 % confidence bounds) were observed with this sample size (Fig. 5 (Left)). By design of the method, the code simulations of the reference sequence 12 result in 158 estimates of the time when the PCT exceeds 1477 K. These estimates are passed through the expression (1) for the evaluation of the core damage frequency. The obtained values range from 6760s to 13200s after correction for the 10 minutes delay (from [2]) for the latest possible SI injection time to prevent core failure.

The cumulative distribution function of failure probability of power recovery is presented in Fig. 5 (Right). The analysis has been applied to three different cases: Case "wi_pp" including all the 13 parameters; Case "wo_pp" with 9 parameters excluding the physical model variabilities; Case "wo_accu" with 11 parameters excluding the variability in the accumulator parameters. As can be seen, propagating uncertainty in physical parameters yields a relatively similar distribution to that without propagating physical parameters uncertainty. The mean values of these two distributions are 0.075 and 0.078, respectively. On the other hand, the distribution without propagating uncertainty in the accumulator parameters increases the mean value up to 0.086, which hints at the fact that the accumulator parameters have more overall impact on the failure probability distribution than the physical parameters.
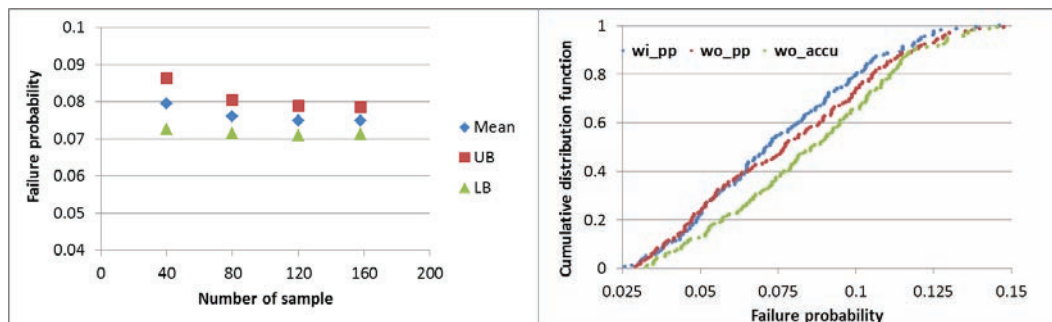

Figure 5. Left: Convergence study for the mean of failure probability; Right: Cumulative distribution of failure probability of power recovery for three different cases.

The core damage frequency for each sample i of the accident sequence is calculated by multiplying the initial event frequency of LOSP by the failure probabilities of the emergency power system and the AFWS, and corrected for the no pump seal failure probability as follows:.

$$CDF(i) = P_{IE-LOSP} \times P_{EPS} \times P_{L1-SBO} \times (1 - P_{SL-S}) \times P_{FPR}(t_i - 10min) \tag{4}$$

Based the on probabilities listed in Table I, the mean CDF of the reference sequence (sequence 12 in Fig. 1 (bottom)) is 2.06E-6. As shown in Table V, the 5% and 95% tile values of the CDF of sequence 12 are 8.81E-7 and 3.27E-6, respectively. The CDF without considering uncertainties (using base case values of the parameters in Table IV) is 3.36E-6. Compared to the CDF with uncertainties, the base case CDF without uncertainties is 1.6 times larger. This implies that the CDF estimate is slightly biased in light of the assumed uncertainties. However, the CDF estimate of sequence 12 from the PSA report [9, 10] is 1.7E-5. The latter is a more conservative estimate compared to this more realistic case study where the power recovery failure probability decreases as function of time.

Table V: Core Damage Frequency for the reference sequence.

	Present evaluation	Ref. [9] (reference PSA)
Without uncertainty propagation	3.36E-6	1.7E-5
With uncertainty propagation	(8.81E-7, 2.06E-6, 3.27E-6)	

4.2.2. Ranking of the uncertain parameters

In order to rank the uncertain parameters both Pearson and Spearman correlation coefficients have been used. For each parameter, the correlation coefficients r_{XY} and ρ with the CDF are calculated using equations (2) and (3), respectively. The resulting Pearson's and Spearman correlation coefficients for each uncertain input parameter are presented in Table VI. These coefficients provide a measure of how much each input parameter is correlated to the output variability. In the table, the larger the absolute value of the coefficient value, the higher the rank.

According to the correlation coefficients values in Table VI, interfacial drag (pre-CHF), axial offset and SG initial liquid mass are the high ranking parameters. The next six tabulated parameters are weakly correlated and last three parameters show negligible correlation to the output parameter. One can note that the initial water volume of accumulator shows weak correlation to the CDF, which somehow contradicts the results discussed in Section 3, where the accumulator parameters were found to affect the CDF distribution more significantly than the physical parameters (including the top-ranked pre-CHF drag).

To clarify this result, we visualize in Fig. 6 the positions of the 16 (10% of total sample) highest and lowest values of three highly correlated parameters according to the ranking of CDF value (from highest to lowest). The three top parameters are negatively correlated which means lowest values (blue bar) should be located in the upper end and highest values (red bar) in the lower end of the CDF value distribution. However, the colored bars for the three input parameters showed relatively mixed distributions, as a result of the small correlation coefficient values (not higher than 0.308, in amplitude).

We select two cases marked with a black bar (corresponds to sample 127 and 157) in Fig. 6 where the variability from the mean value is significant for the SG initial mass inventory parameter but not for the other two top-ranked parameters. The sample 157 is rightly placed in the lower end of the CDF values due to its high value of SG mass inventory (red bar). The location of the sample 127 is less evident, since the SG mass inventory is very low (blue bar), which contradicts the negative correlation to the CDF.

Table VI. Ranking of the uncertain parameters for their correlation with the CDF.

| Parameters	Pearson		Spearman	
	r	Rank	ρ	Rank
Interfacial drag coefficient in pre-CHF flow regime	-0.308	1	-0.281	2
Axial offset	-0.261	2	-0.284	1
SG initial liquid mass	-0.231	3	-0.211	3
Decay heat	0.138	4	0.133	4
Feed and bleed actuation delay	-0.111	5	-0.112	5
Initial power	0.110	6	0.095	6
Pressurizer safety valve section	-0.102	7	-0.076	8
Interfacial drag coefficient in bubbly flow regime	0.091	8	0.085	7
Wall to vapor heat transfer coefficient	0.058	9	0.057	10
Initial water volume of accumulators	-0.032	10	-0.068	9
Pressure loss coefficient of accumulators	0.005	11	0.000	13
SG PORV setpoint pressure	0.003	12	0.020	11
Nucleate boiling heat transfer coefficient	0.000	13	0.000	12
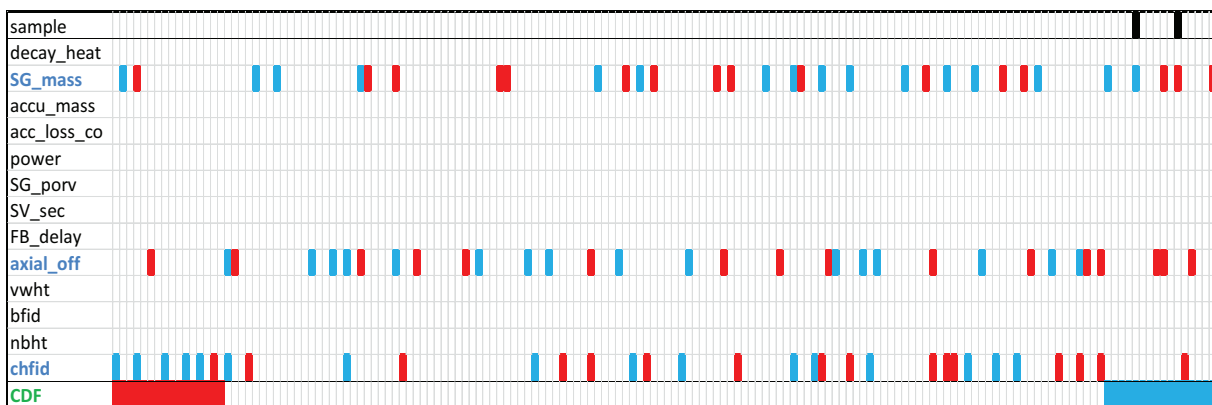
Figure 6. Position of 10%-highest (red) and 10%-lowest (blue) values for three highly correlated parameters based on ranked CDF value (Pearson)

The PCT history for these two cases is compared to the base case PCT in Fig. 7. One can see that the PCT in the two sampled cases experiences an erratic evolution after the accumulators started to discharge. This was not observed in the reference base case, and in most of the samples that resulted in low core failure probabilities. The erratic PCT evolution relates to the intermittent injection from the accumulators (see accumulator level in Fig. 7 (left)). Thus, accumulator injection starts when the primary system pressure goes below the accumulator pressure, and the condensation at the injection point leads to rapid depressurization which in turn sucks additional water from the accumulators. The water injection burst leads to the rise of the core water level which brings about stronger steam vaporization and the primary pressure goes up again (Fig. 7 (right)). This prevents accumulator injection for some time until the primary pressure goes down again thanks to the ventilation through the PZR PORVs. This cyclic behavior is repeated until the accumulators are emptied or sufficiently depressurized.

The accumulator injection cycles are difficult to predict for a given sequence sample, as indicated by the low correlation coefficient values for the accumulator parameters in Table VI. This may stem from effects of non-selected important epistemic parameters (e.g. uncertainty in the condensation models, or accumulator model options) as well as from combined interactions of uncertain parameters, as

demonstrated for the latter by the similar PCT results for the samples 127 and 157 despite very different initial SG mass inventories.
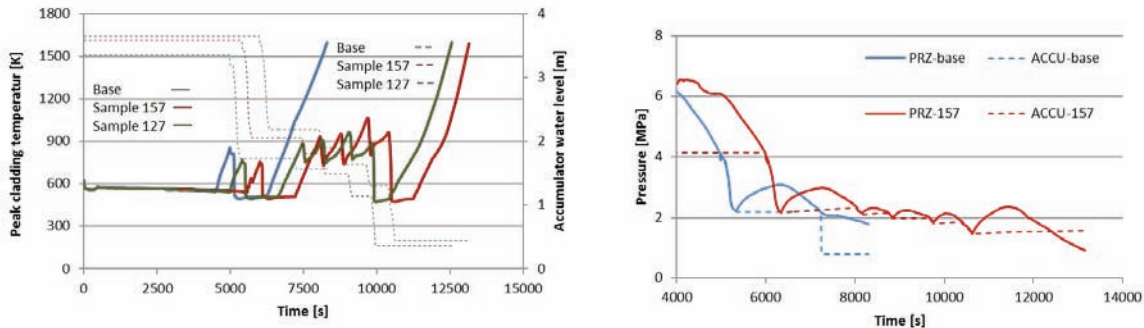

Figure 7. Peak cladding temperature and accumulator level evolution (left); Pressurizer and accumulator pressure history (right).

5. CONCLUSIONS

In this study, a sensitivity analysis of a set of selected candidate parameters has been carried out based on an SBO sequence of the Zion reactor involving loss of AFW system followed by failure to recover power supply for the FB mode. The existing TRACE Zion MBLOCA input model has been adapted for this analysis. Thirteen candidate uncertain parameters have been selected, including I/B conditions and physical model epistemic uncertainties. The input parameters have been considered to be random variables with associated bounds (upper and lower limits) derived from own judgement (CSNI Task Group SM2A, and the authors).

The uncertainties associated with these input parameters have been propagated to determine the variability in the failure probability and corresponding CDF of the selected sequence. The results indicated that the mean of the CDF estimate was 1.6 times higher than the base case estimate without uncertainties. Moreover, the mean CDF with the presented risk model has been found to be approximately 8 times lower than the reference CDF where the failure probabilities of power recovery and of FB actuation were conservatively decoupled.

Moreover, the candidate uncertain parameters have been compared and ranked following their Pearson and Spearman correlation coefficients with the CDF. Both methods indicated the interfacial drag (pre-CHF), the core axial power distribution and the SG mass inventory as the most prominent parameters. However in this case study, it was observed that a non-negligible proportion of the output variability was in fact related to the accumulator parameters, which were characterized by very low correlation coefficient values.

The inability for the rank correlation methods to capture the influence of the accumulators is related to the complex (non-monotonic) interaction between the accumulators and the primary system during the passive accumulator discharge phase, which involves in particular condensation at the accumulator injection point, nitrogen expansion in the accumulator dome and ingress into the primary system, void distribution in the core and the rest of the primary circuit. These phenomena can be affected by interactions of the selected parameters, which could not be captured with the correlation coefficients.

This case study shows that accurate PSA methodologies based on DET framework or surrogate models will require more advanced sensitivity analysis methods as part of the selection of the influential parameters to the CDF variability. As a recent example, the efficacy of the Morris global screening

method has been demonstrated in [15] where it has been shown that parameter interactions can be of high relevance for the determination of the heater rods temperature history during a reflood experiment.

ACKNOWLEDGMENTS

REFERENCES

1. R. R. Sherry, J. R. Gabor, S. M. Hess, "Pilot application of risk informed safety margin characterization to a total loss of feedwater event," Reliability Engineering and System Safety, 117, pp. 65-72 (2013).
2. F. Fouet, P. Probst, J.M. Lanore, "Application of SMAP Methodology to a 10% power up-rate for Zion NPP SBO Transient," PHYSOR – Advances in Reactor Physics to Power the Nuclear Renaissance, Pittsburgh, Pennsylvania, USA, May 9-14 (2010)
3. T.W. Kim, V.N. Dang, M.A. Zimmermann, A. Manera, "Quantitative evaluation of change in core damage frequency by postulated power uprate: Medium-break loss-of-coolant-accidents," *Annals of Nuclear Energy*, **47**, pp. 69-80 (2012).
4. N. Siu, " Risk Assessment for Dynamic Systems: An Overview," *Reliability Engineering and System Safety*, **43**, pp.43-73 (1994).
5. P. E. Labeau, C. Smidts, S. Swaminathan, "Dynamic Reliability: Towards an Integrated Platform for Probabilistic Risk Assessment", *Reliability Engineering and System Safety*, **68**, pp.219-254 (2000).
6. E. Zio, N. Pedroni, G Apostolakis, " Estimation of the failure probability of a thermal-hydraulic passive system by means of Artificial Neural Networks and quadratic Response Surfaces," *European Safety and RELiability (ESREL) 2010 Conference,* pp.714 -721(2010).
7. Y. J. Cho, T.J. Kim, H.G. Lim, G. C. Park, "Effect of uncertainties in best-estimate thermal hydraulic analysis on core damage frequency for PSA," *Nuclear Engineering and Design*, **240**, pp. 4021–4030 (2010).
8. U. S. Nuclear Regulatory Commission, TRACE V5.0 Theory Manual: Field Equations, Solution Methods, and Physical Models (2012).
9. Safety Margin Assessment and Application – Final Report, NEA/CSNI/R(2011)3, Committee on the Safety of Nuclear Installations (CSNI), Nuclear Energy Agency, Paris, France, 2011.
10. M. B. Sattison, K. W. Hall, "Analysis of core damage frequency: Zion, unit 1 internal events", US NRC, NUREG/CR-4550, EGG-2554, Vol. 7, Rev. 1. (1990).
11. BEMUSE phase IV report, "Simulation of a LB-LOCA in ZION nuclear power plant", Main NEA/CSNI/R(2008)6/VOL1-3.
12. U. S. Nuclear Regulatory Commission, TRACE Pressurized Water Reactor Modelling Guidance (2012).
13. H. Tochihara, "Simple Functional Method for Calculating Axial Power Distribution of PWR Core," Journal of Nuclear Science and Technology, 19:6, 449-459 (1982).
14. K. D. Rao, H. S. Kushwaha, A. K. Verma and A. Srividya, "A New Uncertainty Importance Measure in Fuzzy Reliability Analysis," *International Journal of Performability Engineering*, **5**, No. 3, pp. 219-226 (2009).
15. D. Wicaksono, O. Zerkak, A. Pautz, "A methodology for global sensitivity analysis of transient code output applied to a reflood experiment model using TRACE," accepted for the publication, The 16th International Topical Meeting on Nuclear Reactor Thermal Hydraulics (NURETH-16), Chicago, USA, 2015.